



HAL
open science

A COMPARISON OF BEAM MODELS FOR THE DYNAMICS OF RAILWAY TRACKS ON A NON-UNIFORM VISCOELASTIC FOUNDATION

Benjamin Claudet, Denis Duhamel, Gilles Foret, Tien Hoang, Jean-Luc Pochet, Francis Sabatier

► **To cite this version:**

Benjamin Claudet, Denis Duhamel, Gilles Foret, Tien Hoang, Jean-Luc Pochet, et al.. A COMPARISON OF BEAM MODELS FOR THE DYNAMICS OF RAILWAY TRACKS ON A NON-UNIFORM VISCOELASTIC FOUNDATION. ICSV27, Jul 2021, Ostrava, Czech Republic. hal-03689417

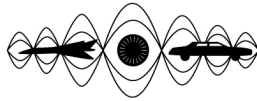
HAL Id: hal-03689417

<https://hal.science/hal-03689417v1>

Submitted on 7 Jun 2022

HAL is a multi-disciplinary open access archive for the deposit and dissemination of scientific research documents, whether they are published or not. The documents may come from teaching and research institutions in France or abroad, or from public or private research centers.

L'archive ouverte pluridisciplinaire **HAL**, est destinée au dépôt et à la diffusion de documents scientifiques de niveau recherche, publiés ou non, émanant des établissements d'enseignement et de recherche français ou étrangers, des laboratoires publics ou privés.



Annual Congress of the International Institute of Acoustics and Vibration (IIAV)

A COMPARISON OF BEAM MODELS FOR THE DYNAMICS OF RAILWAY TRACKS ON A NON-UNIFORM VISCOELASTIC FOUNDATION

Benjamin CLAUDET, Denis DUHAMEL, Gilles FORET, Tien HOANG

École des Ponts ParisTech, Champs-sur-Marne, France

e-mail: benjamin.claudet@enpc.fr

Jean-Luc POCHET, Francis SABATIER

Eurotunnel, Coquelles, France

Many numerical or analytical methods have been developed to compute the response of a railway track on a uniform foundation. The rail can then be modelled by different beam models. It was shown that for uniform railway tracks, Euler beam model and Timoshenko beam model give close results. In the case of damaged railway track components, the defaults can cause higher displacements of the rail leading to higher shears. Thus, in this case, the Timoshenko beam model can be more interesting. In this paper, a semi-analytical model for a railway track resting on a non-uniform foundation is proposed where the rail is modelled by a Timoshenko beam. Then, the results obtained with Timoshenko beam model and Euler Bernoulli beam model are compared for both a uniform railway track and a damaged railway track.

Keywords: Railway tracks dynamics, Timoshenko beam, Euler beam, Non-uniform foundation

1. Introduction

To compute the dynamics of railway tracks subjected to moving loads, many authors modelled the tracks with a periodically supported beams [1, 2, 3, 4]. Some of them [3, 4] gave analytical results for describing the dynamics of a homogeneous railway track. In many cases, for instance tracks with damaged supports or transition zones, the track can not be considered as homogeneous. To compute the dynamics of this type of tracks, many authors [5, 6] used fully numerical models. Hoang *et al* developed an analytical method to compute the behaviour of a beam resting on a non-uniform viscoelastic foundation where the supports are modelled as mass-spring-dampers systems and an Euler beam model is used [7].

Contrary to Timoshenko beams, when an Euler beam is deformed the sections remain perpendicular to the neutral axis. Hoang *et al* showed [8] that for homogeneous tracks, Euler and Timoshenko beam models give close results. In the non-uniform case, especially for a damaged track, displacements have a larger amplitude, leading to higher shears. Thus, in this case, Timoshenko beam model can be more interesting.

This article develops the analytical method proposed by Hoang *et al* [7] for Timoshenko beams. Results obtained with the two beam models are then compared on a uniform track and a damaged track.

2. Track model

2.1 Supports description

A rail supported by periodic supports (sleepers) is modelled. Each support contains two elastic stages: the rail pad and an elastic stage under the sleeper (see figure 1). In the examples used thereafter, a ballastless track is considered. Therefore the under-sleeper elastic stage can be reduced to the under-sleeper pad. For ballasted track this second elastic stage must take into account the ballast stiffness too. The supports are supposed punctual and are modelled as mass-spring-dampers systems.

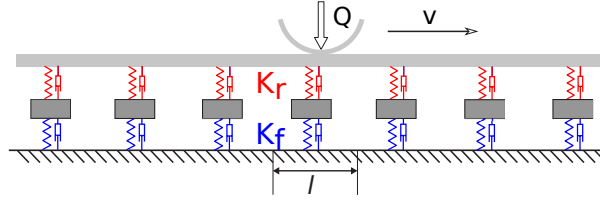


Figure 1: Model of the periodically supported beam.

In the frequency domain, the dynamic stiffness of the two elastic stages is given by (1) where k is the stiffness and ξ the damping coefficient and the subscript r is for the rail pad and f for the foundation or the under-sleeper pad.

$$\begin{cases} K_r = k_r + i\omega\xi_r \\ K_f = k_f + i\omega\xi_f - \omega^2 M \end{cases} \quad (1)$$

Combining the two precedent equations, the support dynamic stiffness is given by $K_s = (K_r^{-1} + K_f^{-1})^{-1}$.

2.2 Timoshenko beam model

In this paper, the rail is modelled by a Timoshenko beam of constant section S , with a flexion rigidity EI and subjected to an external force F . The Timoshenko beam model was introduced [9] to take into account shear deformation and rotational bending effects in beam flexions. In that aim, a degree of freedom θ describing the section angle is added to the Euler beam model. The dynamic equation of a Timoshenko beam's flexion are given in the frequency domain by (2).

$$\begin{cases} \kappa SG \partial_x \hat{\theta} = \kappa SG \partial_x^2 \hat{w} + \rho S \omega^2 \hat{w} + \hat{F} \\ -\kappa SG \partial_x \hat{w} = EI \partial_x^2 \hat{\theta} - (\kappa SG - \rho I \omega^2) \hat{\theta} \end{cases} \quad (2)$$

The shear modulus G is a material property defined as the ratio between shear stress and shear rate. The Timoshenko shear coefficient κ is a parameter which depends on the section's geometry. In the limit $\frac{EI}{\kappa L^2 SG} \ll 1$ -ie. for beam with a high shear rigidity compared to his flexion rigidity- the Timoshenko beam model converges to the Euler beam model.

Considering only the rail deflexion \hat{w} (2), can be reduced to:

$$EI [\partial_x^2 + \lambda_1^2] [\partial_x^2 - \lambda_2^2] \hat{w} = \left[1 - \frac{EI}{\kappa SG} \partial_x^2 - \frac{\rho I \omega^2}{\kappa SG} \right] F(x, \omega) \quad (3)$$

With,

$$\lambda_{1,2}^2 = \sqrt{\frac{\omega^4}{4} \left(\frac{\rho I}{EI} - \frac{\rho S}{\kappa SG} \right)^2 + \frac{\rho S \omega^2}{EI}} \pm \frac{\omega^2}{2} \left(\frac{\rho I}{EI} + \frac{\rho S}{\kappa SG} \right) \quad (4)$$

3. Periodical support system

The supports are supposed to be periodically distributed. The period has a length $L = ml$ where m is an integer and l is the spacing between two consecutive supports. The train is modelled by a set of constant moving loads $\{Q_j\}$ characterized by the distances $\{D_j\}$. The train's speed v is constant. It is also supposed that the reaction forces in a period are the same as the reaction forces in the previous period with a temporal delay of $\frac{L}{v}$ (so-called "periodic condition"). Calling R_k the reaction force due to the support k , (5) is obtained.

$$\forall (n, p) \in \mathbb{Z}^2, R_{nm+p}(t) = R_p \left(t - \frac{nL}{v} \right) \quad (5)$$

Thus, in the temporal domain the force F follows:

$$F(x, t) = \sum_{n \in \mathbb{Z}} \sum_{p=0}^{m-1} R_p \left(t - \frac{x - pl}{v} \right) \delta(x - pl - nL) - \sum_{j=1}^K Q_j \delta(x - D_j - vt) \quad (6)$$

And, in the frequency domain, \hat{F} :

$$\begin{aligned} \hat{F}(x, \omega) &= \sum_{n \in \mathbb{Z}} \sum_{p=0}^{m-1} \hat{R}_p(\omega) e^{-i\omega \frac{x-pl}{v}} \delta(x - nL - pl) - \sum_{j=1}^K \frac{Q_j}{v} e^{-i\omega \frac{x+D_j}{v}} \\ &= e^{-i\omega \frac{x}{v}} \left(\sum_{n \in \mathbb{Z}} \sum_{p=0}^{m-1} \hat{R}_p(\omega) e^{i\omega \frac{pl}{v}} \delta(x - nL - pl) - \sum_{j=1}^K \frac{Q_j}{v} e^{-i\omega \frac{D_j}{v}} \right) \end{aligned} \quad (7)$$

$\hat{F}(x, \omega) e^{i\omega \frac{x}{v}}$ is L periodic and we have:

$$\frac{1}{L} \int_{-L/2}^{L/2} \hat{F}(x, \omega) e^{i\omega \frac{x}{v}} e^{-2i\pi n \frac{x}{L}} dx = \frac{1}{L} \sum_{p=0}^{m-1} \hat{R}_p(\omega) e^{i(\frac{\omega}{v} - \frac{2\pi n}{L})pl} - \frac{\delta_{0n}}{v} \sum_{j=1}^K Q_j e^{-i\omega \frac{D_j}{v}} \quad (8)$$

Thus, using the method described in [8], (9) is obtained.

$$\hat{w}(x, \omega) = \sum_{p=0}^{m-1} \hat{R}_p(\omega) e^{i\omega \frac{pl-x}{v}} \eta(pl - x, \omega) - \eta(0, \omega) \mathcal{Q}(\omega) e^{-i\omega \frac{x}{v}} \quad (9)$$

Where,

$$\begin{aligned} \eta(x, \omega) &= \frac{e^{i\omega \frac{x}{v}}}{2EI(\lambda_1^2 + \lambda_2^2)} \left[\frac{C_1 \sin \lambda_1(L-x) + e^{-i\omega \frac{L}{v}} \sin \lambda_1 x}{\lambda_1 \cos L\lambda_1 - \cos \frac{\omega L}{v}} - \frac{C_2 \sinh \lambda_2(L-x) + e^{-i\omega \frac{L}{v}} \sinh \lambda_2 x}{\lambda_2 \cosh L\lambda_2 - \cos \frac{\omega L}{v}} \right] \\ \mathcal{Q}(\omega) &= \frac{\tilde{p}_0 L}{v} \eta(0, \omega)^{-1} \sum_{j=1}^K Q_j e^{-i\omega \frac{D_j}{v}} \\ C_{1,2} &= 1 - \frac{\rho I \omega^2 \mp EI \lambda_{1,2}^2}{\kappa S G} \\ \tilde{p}_0 L &= \frac{x S G - \rho I \omega^2 + EI \frac{\omega^2}{v^2}}{x S G (EI \frac{\omega^4}{v^4} - \rho S \omega^2) - \rho S I (x G + E - \rho v^2) \frac{\omega^4}{v^2}} \end{aligned} \quad (10)$$

Evaluated at $x = 0$, the equation (9) gives :

$$\hat{w}(0, \omega) = \sum_{p=0}^{m-1} \hat{R}_p(\omega) e^{i\frac{\omega pl}{v}} \eta_p(\omega) - \eta_0(\omega) \mathcal{Q}(\omega) \quad (11)$$

The equation (11) is very similar to the equation given in [7]. The differences between the two beam models are contained in the exact expression of $\eta_p(\omega) = \eta(pl, \omega)$ and \tilde{p}_0 . Indeed, the Euler beam model can be obtained by taking the limit $G \rightarrow +\infty$ which leads to $C_1 = C_2 = 1$ and $\lambda_{1,2} = \sqrt{(\rho S \omega^2)/(EI)}$. The rest of the method remains identical. Therefore, only the key steps are reminded in the following.

From (9), remarking $\eta_{m+p-q} = \eta_{p-q}$, for $x = ql$ ($q \in \mathbb{Z}$) it can be shown that:

$$\hat{w}(ql, \omega) e^{i\frac{\omega ql}{v}} = \sum_{p=0}^{m-1} \hat{R}_p(\omega) e^{i\frac{\omega pl}{v}} \eta_{(p-q)} - \eta_0 \mathbf{Q}_e(\omega) \quad (12)$$

Defining \mathbf{w}_q and \mathbf{R}_q as in (13), (14) and (15) are obtained.

$$\begin{cases} \mathbf{w}_q(t) = w_r \left(ql, t - \frac{ql}{v} \right) \\ \mathbf{R}_q(t) = R_q \left(t - \frac{ql}{v} \right) \end{cases} \quad (13)$$

$$\hat{\mathbf{w}}_q(\omega) = \sum_{p=0}^{m-1} \hat{\mathbf{R}}_p(\omega) \eta_{(p-q)} - \eta_0 \mathbf{Q}_e(\omega) \quad (14)$$

$$\begin{pmatrix} \eta_0 & \eta_1 & \cdots & \eta_{m-1} \\ \eta_{m-1} & \eta_0 & \cdots & \eta_{m-2} \\ \vdots & \vdots & \ddots & \vdots \\ \eta_1 & \eta_2 & \cdots & \eta_0 \end{pmatrix} \begin{pmatrix} \hat{\mathbf{R}}_0 \\ \hat{\mathbf{R}}_1 \\ \vdots \\ \hat{\mathbf{R}}_{m-1} \end{pmatrix} = \eta_0 \mathbf{Q}_e \begin{pmatrix} 1 \\ 1 \\ \vdots \\ 1 \end{pmatrix} + \begin{pmatrix} \hat{\mathbf{w}}_0 \\ \hat{\mathbf{w}}_1 \\ \vdots \\ \hat{\mathbf{w}}_{m-1} \end{pmatrix} \quad (15)$$

Writting $\underline{\mathbf{1}} = {}^t(1, \dots, 1)$, (15) can be rewritten in a reduced form:

$$\underline{\underline{\mathbf{C}}} \hat{\underline{\underline{\mathbf{R}}}} = \eta_0 \mathbf{Q}_e \underline{\mathbf{1}} + \hat{\underline{\underline{\mathbf{w}}}} \quad (16)$$

(16) links the deflexion of the beam with the reaction forces. This relationship only comes from the periodicity of the problem and the beam behaviour. Another relationship is needed to close the problem. This other relationship comes from the support stiffness and can be written as in (17).

$$\hat{\underline{\underline{\mathbf{w}}}} = -\underline{\underline{\mathbf{D}}} \hat{\underline{\underline{\mathbf{R}}}} \quad (17)$$

Where $\underline{\underline{\mathbf{D}}} = \text{diag}(1/K_{s0}, 1/K_{s1}, \dots, 1/K_{s(m-1)})$ and $1/K_{sp}$ is the stiffness of the support p . Combining (17) and (16), (18) is obtained.

$$\hat{\underline{\underline{\mathbf{R}}}} = \mathbf{Q}_e \underline{\underline{\mathbf{A}}}^{-1} \underline{\mathbf{1}} \quad (18)$$

Where $\underline{\underline{\mathbf{A}}} = \eta_0^{-1} (\underline{\underline{\mathbf{C}}} + \underline{\underline{\mathbf{D}}})$.

$\underline{\underline{\mathbf{A}}}$ is a $m \times m$ matrix which depends on the frequency and whose computation is fast and simple. However, when one of the stiffness is equal to zero (lack of a support, broken support) this matrix is not well-defined. To study these cases, an iterative method is developed in [7] and reminded in the next part.

4. Iterative resolution for non-uniform tracks

The beam considered has a local part where the supports have different behaviours (reinforced or damaged) from normal supports. This local different part is included in a larger zone of length $L = ml$ (see figure 2). This zone is taken large enough so that the central different part has no effect on the borders of the large zone. This hypothesis makes possible to consider the track periodic and therefore to use the results obtained with periodic support systems. On the other hand, this hypothesis should be verified *aposteriori*.

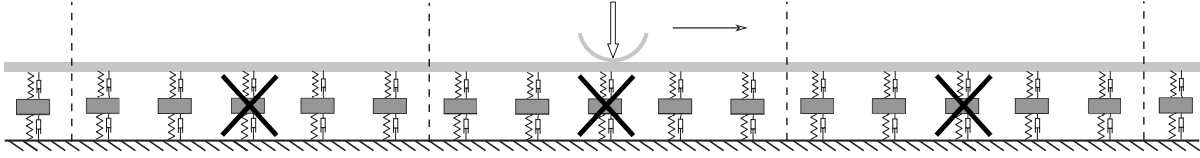


Figure 2: Periodically supported beam with one damaged support. In this illustration, the period contains $m = 5$ supports, one of them being broken.

(14) and (15) represent a convolution product plus a constant part. Therefore it can be rewritten :

$$\hat{\underline{\mathbf{w}}} = \underline{\eta} \star \hat{\underline{\mathbf{R}}} - \eta_0 \underline{\mathbf{Q}}_e \underline{\mathbf{I}} \quad (19)$$

Performing a discrete Fourier transform defined by (20) on (19) gives (21)

$$\forall f, \mathcal{F}_q \{f\} = \sum_{p=0}^{m-1} e^{i2\pi \frac{pq}{m}} f_p \quad (20)$$

$$\mathcal{F}_q \left\{ \hat{\underline{\mathbf{R}}} \right\} = \kappa_q \mathcal{F}_q \left\{ \hat{\underline{\mathbf{w}}} \right\} + m \underline{\mathbf{Q}}_e \delta_{1q} \quad (21)$$

Where $\underline{\mathbf{Q}}_e = \eta_0 \underline{\mathbf{Q}}_e / \mathcal{F}_0 \left\{ \hat{\underline{\eta}} \right\}$ and $\kappa_q = \left(\mathcal{F}_q \left\{ \hat{\underline{\eta}} \right\} \right)^{-1}$.

The discrete Fourier transform $\mathcal{F}_q \left\{ \hat{\underline{\eta}} \right\}$ is given by :

$$\mathcal{F}_q \left\{ \hat{\underline{\eta}} \right\} = \frac{1}{2EI (\lambda_1^2 + \lambda_2^2)} \left[\frac{C_1}{\lambda_1} \frac{\sin \lambda_1 l}{\cos l \lambda_1 - \cos \left(\frac{\omega l}{v} + \frac{2\pi q}{m} \right)} - \frac{C_2}{\lambda_2} \frac{\sinh \lambda_2 l}{\cosh l \lambda_2 - \cos \left(\frac{\omega l}{v} + \frac{2\pi q}{m} \right)} \right] \quad (22)$$

As in the previous part, the problem closure is given by the support stiffness. This relationship can be written :

$$\begin{aligned} \hat{\underline{\mathbf{R}}} &= -\underline{\mathbf{K}} \hat{\underline{\mathbf{w}}} \\ &= -\left(\underline{\mathbf{K}} - K_{sn} \underline{\mathbf{I}} \right) \hat{\underline{\mathbf{w}}} - K_{sn} \hat{\underline{\mathbf{w}}} \\ &= \tilde{\underline{\mathbf{R}}} - K_{sn} \hat{\underline{\mathbf{w}}} \end{aligned} \quad (23)$$

Where $\underline{\mathbf{K}} = \text{diag}(K_{s0}, K_{s1}, \dots, K_{s(m-1)})$ and K_{sn} is the stiffness of the supports in a normal zone. The iteration procedure proposed in [7] is:

$$\begin{cases} \tilde{\underline{\mathbf{R}}}^n = -\left(\underline{\mathbf{K}} - K_{sn} \underline{\mathbf{I}} \right) \hat{\underline{\mathbf{w}}}^n \\ \hat{\underline{\mathbf{w}}}^{n+1} = \mathcal{F}^{-1} \left(\frac{1}{\kappa_q + k_{nd}} \left[\mathcal{F}_q \left(\tilde{\underline{\mathbf{R}}}^n \right) + m \underline{\mathbf{Q}}_e \delta_{1q} \right]_{0 \leq q < m} \right) \end{cases} \quad (24)$$

The initial values are given by the results for a uniform track: they follow (25).

$$\hat{\underline{\mathbf{w}}}^0 = \frac{\underline{\mathbf{Q}}_e}{\kappa_0 + K_{sn}} \underline{\mathbf{I}} \quad (25)$$

5. Numerical examples

5.1 Periodic track

A periodic track which contains no default is considered. The track parameters are given in Table 1. These parameters correspond to the ballastless track in the Eurotunnel (see [7, 8]). The load is constituted of one wheel with a weight $Q = 100$ kN, moving at a speed $v = 37$ m s⁻¹. As the track is uniform and only a constant moving load is considered, all the support must receive the same load. Therefore the displacement of the rail must be the same above all sleepers with a delay corresponding to the time needed for the load to pass from one sleeper to the others.

Parameter	Symbol	Value
Rail mass	ρS	60 kg m ⁻¹
Rail flexion stiffness	EI	6.38 MN m ²
Rail Timoshenko ratio	κ	0.4
Rail shear modulus	G	8.077 GPa
Train speed	v	37 m s ⁻¹
Charge per wheel	Q	100 kN
Block mass	M	100 kg
Sleeper spacing	l	0.6 m
Railpad stiffness	k_r	192 MN m ⁻¹
Railpad damping	ξ_r	1.97 MN s m ⁻¹
Under-sleeper stiffness	k_f	26.4 MN m ⁻¹
Under-sleeper damping	ξ_f	0.17 MN s m ⁻¹

Table 1: Physical parameters used in the computations.

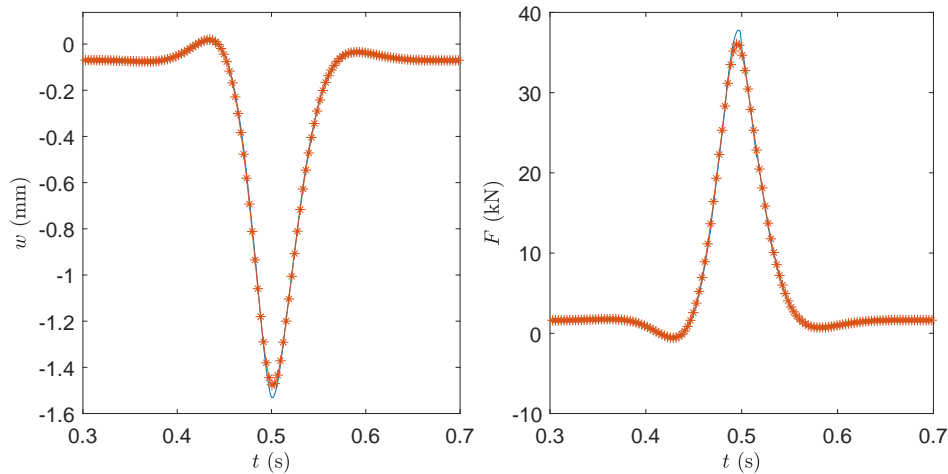


Figure 3: Displacement of the rail above one support (left) and force applied by the support (right) against time for a uniform track. The Timoshenko model results are in continuous line and the Euler model results are represented with line with star markers.

In figure 3 Euler and Timoshenko beam model results are compared. The displacement of one point of the rail (left graph) and the force applied on one support (right graph) are plotted against time. As expected, the Timoshenko beam is a little less rigid than the Euler one. Consequently, both the displace-

ment and the force are larger with a Timoshenko beam. The maximal force computed is 4.5% larger using a Timoshenko beam model (3.5% for the displacement).

5.2 Damaged track

A track containing one damaged support is considered, in this second numerical example. To model this damage, in a conservative approach, the damaged support has no stiffness or damping. As the computation method used is periodic, we choose a period containing 20 healthy supports each side the damaged one ($m = 41$). The number of iterations was fixed to 20 after verifying that doubling this number does not change the results. As the computation only lasts few seconds, no more optimizations were made.

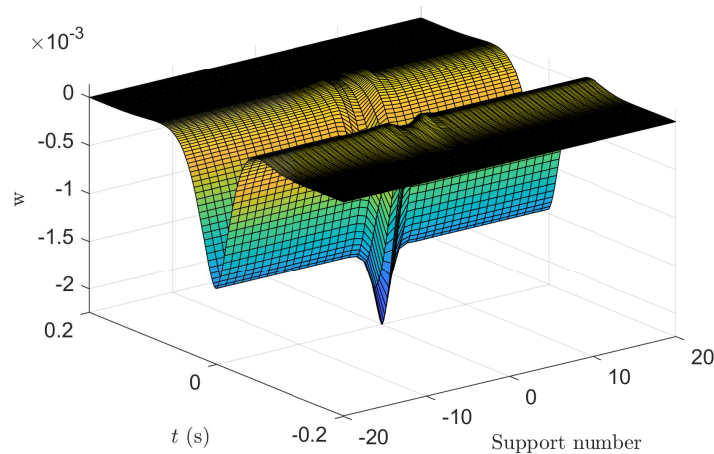


Figure 4: Rail displacement along the rail length against time for a track containing one broken support.

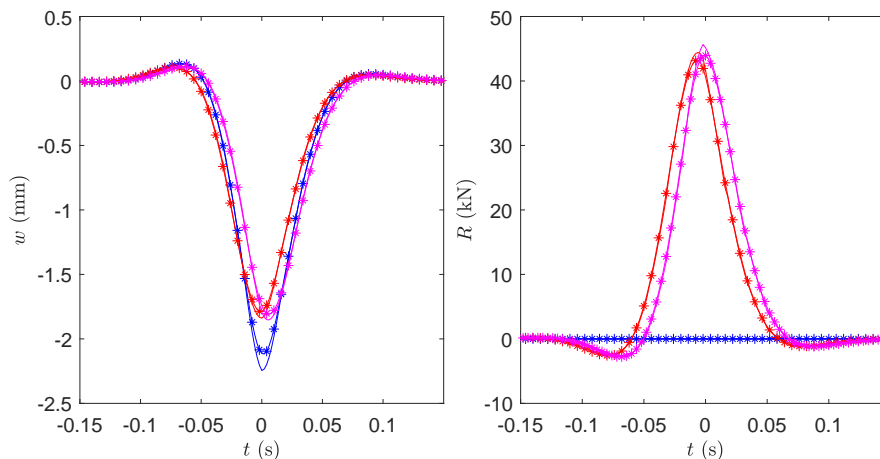


Figure 5: Displacement of the rail above supports (left) and force applied by the supports (right) against time for a damaged track. The Timoshenko model results are in continuous line and the Euler model results are represented with lines with star markers. Damaged support and the two neighbouring supports.

Figure 4 shows the displacement of the rail above the different sleepers. Figure 5 shows the forces and displacement for the damaged support and supports at ± 1.2 m. The difference between Euler and

Timoshenko beam maximum forces is now more than 4.6% near the broken support but for the broken support's displacement, this difference grows up to 6.1%. This proves that the difference between those models is increased for a damaged track. In a case where more supports are damaged or with a higher train speed, this difference is even more important and can not be neglected anymore.

6. Conclusion

Hoang *et al* in [7] proposed a method to compute the dynamics of periodically supported Euler beam on non-uniform railway tracks. In this article, this method was adapted to the Timoshenko beam model. It has been shown [8] that for uniform tracks, the Timoshenko beam model gives different results from Euler beam model and that this difference was growing with the speed and the support stiffness. Applying Hoang *et al* method, it was proved that considering forces this model difference is conserved for a damaged track and significantly increased considering displacements.

REFERENCES

1. Sheng, X., Jones, C. and Thompson, D. J. Responses of infinite periodic structures to moving or stationary harmonic loads, *Journal of Sound and Vibration*, **282** (1-2), 125–149, (2005).
2. Kouroussis, G. and Verlinden, O. Prediction of railway ground vibrations: Accuracy of a coupled lumped mass model for representing the track/soil interaction, *Soil Dynamics and Earthquake Engineering*, **69**, 220–226, (2015).
3. Nordborg, A. Vertical Rail Vibrations: Parametric Excitation, *ACUSTICA· acta acustica*, **84**, 289–300, (1998).
4. Belotserkovskiy, P. On the oscillations of infinite periodic beams subjected to a moving concentrated force, *Journal of Sound and Vibration*, **193** (3), 705–712, (1996).
5. Claudet, B., Hoang, T., Duhamel, D., Foret, G., Pochet, J.-L. and Sabatier, F. Wave Finite Element Method for computing the dynamic response of railway transition zones subjected to moving loads, *Proceedings of the 7th International Conference on Computational Methods in Structural Dynamics and Earthquake Engineering (COMPDYN 2015)*, Athens, pp. 4538–4547, Institute of Structural Analysis and Antiseismic Research School of Civil Engineering National Technical University of Athens (NTUA) Greece, (2019).
6. Arlaud, E., Costa D'aguiar, S. and Balmes, E. Receptance of railway tracks at low frequency: Numerical and experimental approaches, *Transportation Geotechnics*, **9**, 1–16, (2016).
7. Hoang, T., Duhamel, D., Foret, G., Yin, H., Cumunel, G., Joyez, P. and Caby, R. Response of a Periodically Supported Beam on a Non-Uniform Viscoelastic Foundation subject to Moving Loads, Pombo, J. (Ed.), *Proceedings of the Third International Conference on Railway Technology: Research, Development and Maintenance*, Stirlingshire, Scotland, no. April, Civil-Comp Press, (2016).
8. Hoang, T., Duhamel, D. and Foret, G. Dynamical response of a Timoshenko beams on periodical nonlinear supports subjected to moving forces, *Engineering Structures*, **176**, 673–680, (2018).
9. Timoshenko, S. LXVI. On the correction for shear of the differential equation for transverse vibrations of prismatic bars, *The London, Edinburgh, and Dublin Philosophical Magazine and Journal of Science*, **41** (245), 744–746, (1921).